10.1071/CH14205_AC

Australian Journal of Chemistry **2014, 67(12), 1711-1717**

Supplementary Material

Fluorescent analogues of NAMI-A: Syntheses, characterisation, fluorescent properties and preliminary biological studies in human lung cancer cells.

Sumy Antony,[1,2] Jonathan C. Morris,[3] Toby Bell,[2] Tracey Brown,[4] Leone Spiccia,[2] and Hugh H. Harris.[1]

[1] School of Chemistry and Physics, The University of Adelaide, Adelaide SA 5005, Australia

[2] School of Chemistry, Monash University, Clayton, Victoria 3800, Australia

[3] School of Chemistry, University of New South Wales, Sydney, NSW 2052, Australia

[4] Department of Biochemistry and Molecular Biology, Monash University, Clayton, Victoria 3800, Australia.

Instrumentation

A Micromass Platform II Quadrupole Mass Spectrometer was used for obtaining low-resolution electrospray mass spectra (ESI-MS). ^{1}H NMR spectra were measured on Bruker DRX 400 spectrometer. The chemical shifts are reported in parts per million (ppm) relative to signals from the residual protons of the deuterated solvent. *UV-Vis* spectra were recorded in quartz cuvettes using a Cary 300 Bio UV-Vis spectrophotometer. Absolute quantum yields and corrected fluorescence spectra were recorded on solutions at low concentration, which gave an absorbance less than 0.1, in quartz cuvettes using a Cary Eclipse fluorescence spectrophotometer. Analytical HPLC was performed on an Agilent 1260 Infinity HPLC using a Supelco Discovery C5 column. Eluent A, 0.1% (v/v) TFA in water; eluent B, 0.1% (v/v) TFA in CH_3CN; gradient elution, 5% to 75% of eluent B in 25 min, 1.5 mL/min. An xCELLigence cell adhesion impedance system (Roche Applied Science and ACEA Biosciences) was used to carry out cytotoxicity measurements.

Mass Spectra

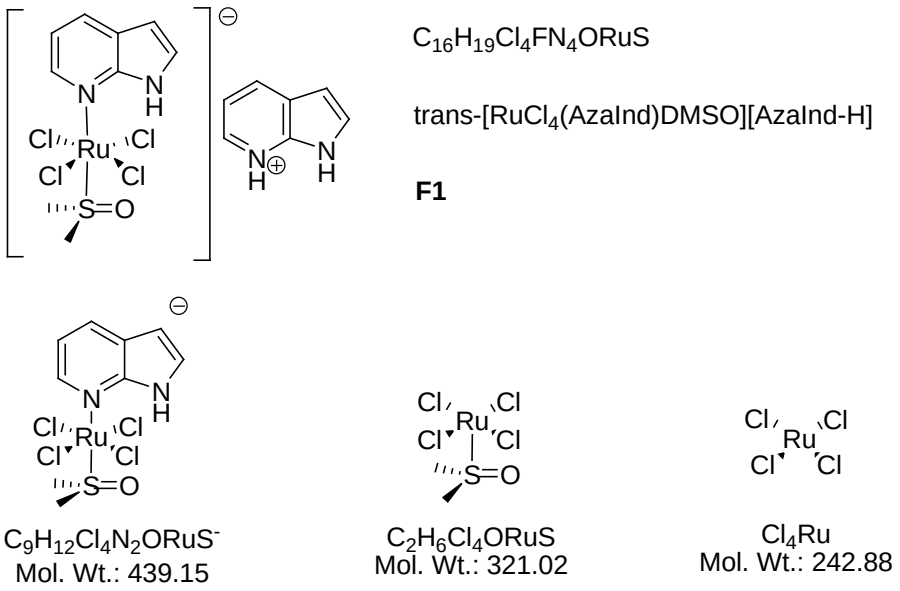

Figure S1: Splitting pattern for **7-azaindolium *trans*-tetrachlorido(7-azaindole)(dimethylsulfoxide)ruthen(III)ate (F1).**

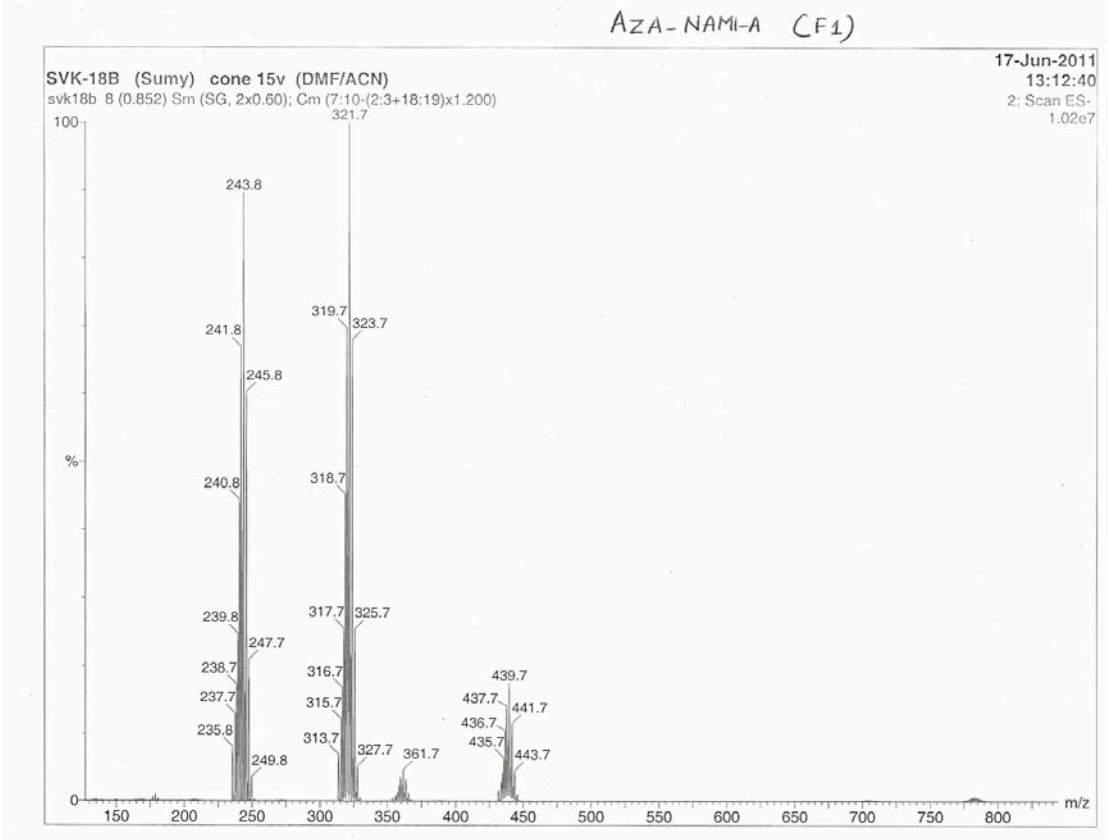

Figure S2: Electrospray mass spectrum (-ve ion) for **F1**; Cone 15V; Solvent – DMF/ACN.

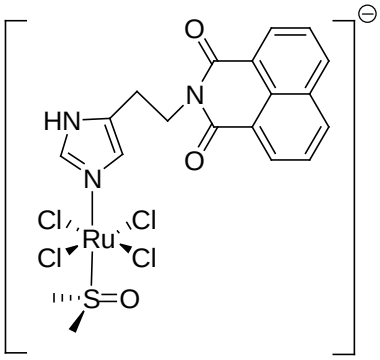

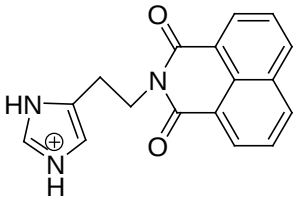

$C_{36}H_{33}Cl_4F_2N_6O_5RuS$

trans-[$RuCl_4$(Hist)DMSO][Hist-H]

F2

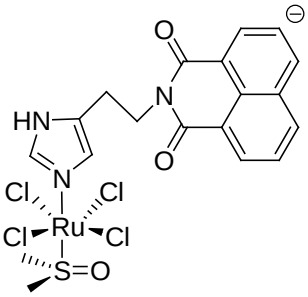

$C_{19}H_{19}Cl_4N_3O_3RuS^-$
Mol. Wt.: 612.32

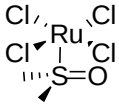

$C_2H_6Cl_4ORuS$
Mol. Wt.: 321.02

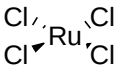

Cl_4Ru
Mol. Wt.: 242.88

Figure S3: Splitting pattern for **N-[histaminedihydrolium]-1,8-naphthalenecarboximidic *trans*-tetrachlorido(dimethylsulfoxide)(N-[histaminedihydro]-1,8-naphthalenecarboximide) ruthen(III)ate (F2)**.

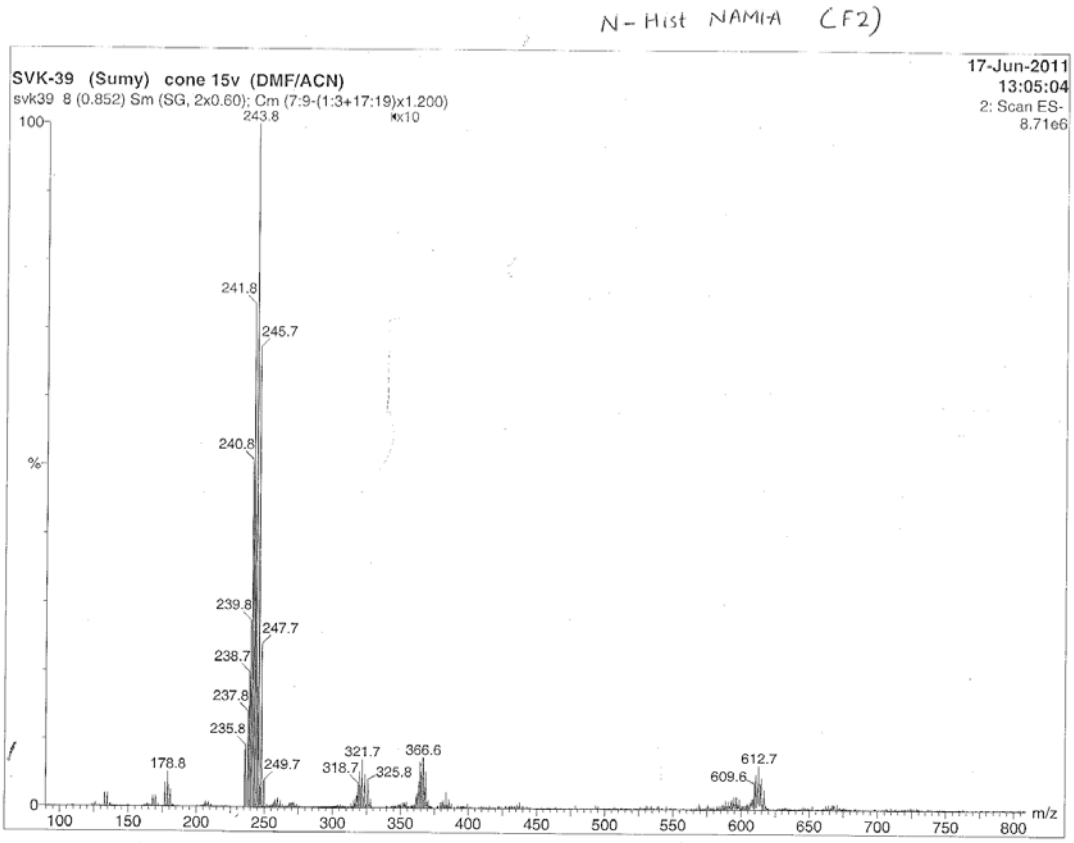

Figure S4: Electrospray mass spectrum (-ve ion) for **F2**; Cone 15V; Solvent – DMF/ACN.

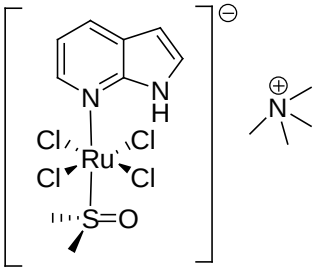

$C_{13}H_{24}Cl_4F_3N_3ORuS$

trans-[$RuCl_4$(AzaInd)DMSO][[$(CH_3)_4N$]

F3

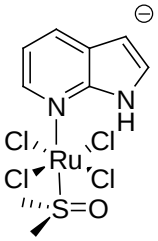

$C_9H_{12}Cl_4N_2ORuS^-$
Mol. Wt.: 439.15

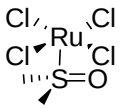

$C_2H_6Cl_4ORuS$
Mol. Wt.: 321.02

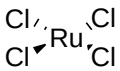

Cl_4Ru
Mol. Wt.: 242.88

Figure S5: Fragmentation pattern for **Tetramethylammonium *trans*-tetrachlorido(7-azaindole)(dimethyl sulfoxide)ruthen(III)ate (F3)**

.

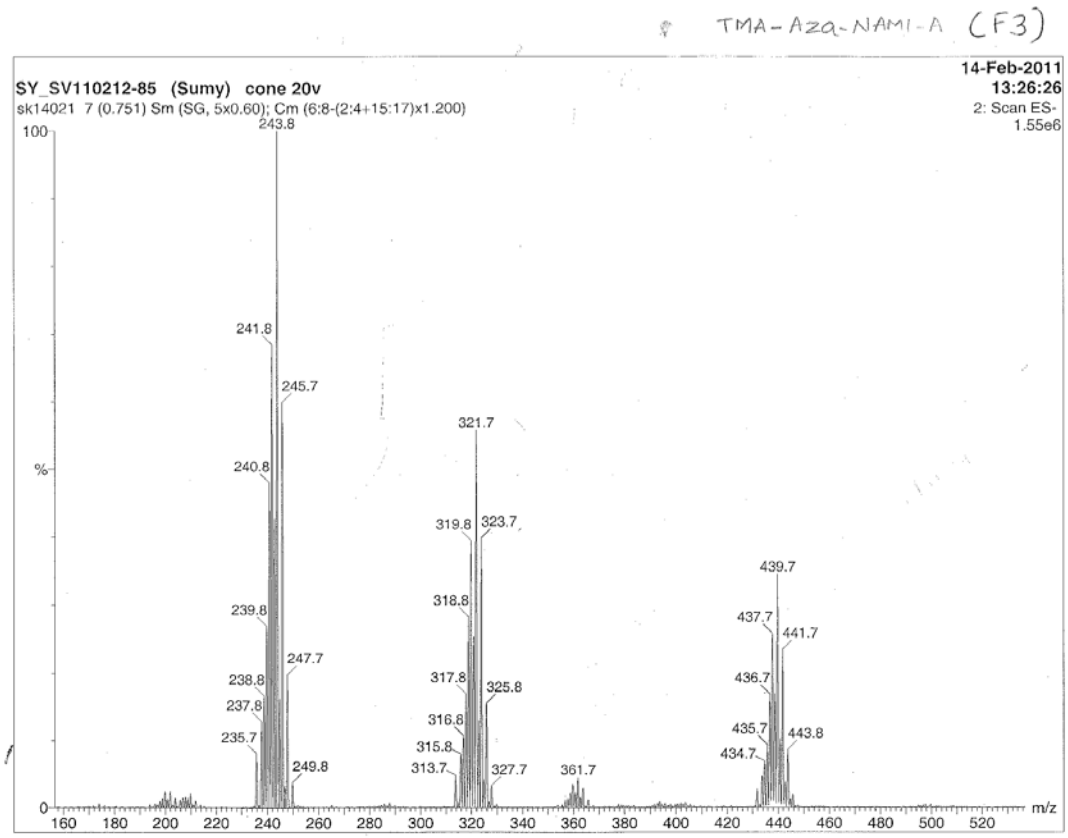

Figure S6: Electrospray mass spectrum (-ve ion) for **F3**; Cone 15V; Solvent – DMF/ACN.

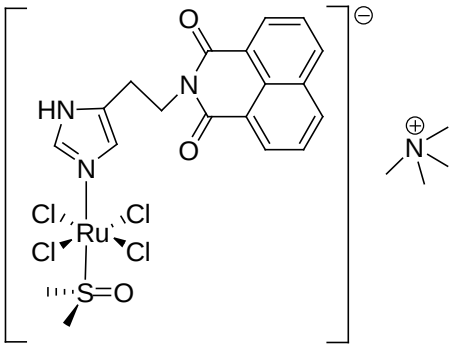

$C_{23}H_{31}Cl_4F_4N_4O_3RuS$

trans-[$RuCl_4$(Hist)DMSO][$(CH_3)_4N$]

F4

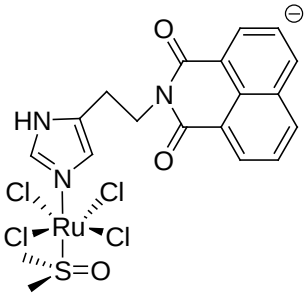

$C_{19}H_{19}Cl_4N_3O_3RuS^-$
Mol. Wt.: 612.32

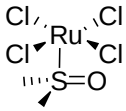

$C_2H_6Cl_4ORuS$
Mol. Wt.: 321.02

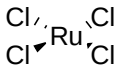

Cl_4Ru
Mol. Wt.: 242.88

Figure S7: Fragmentation pattern for **Tetramethylammonium *trans*-tetrachlorido(dimethylsulfoxide)(N-[histaminedihydro]-1,8-naphthalenecarboximide)ruthen(III)ate (F4)**.

.

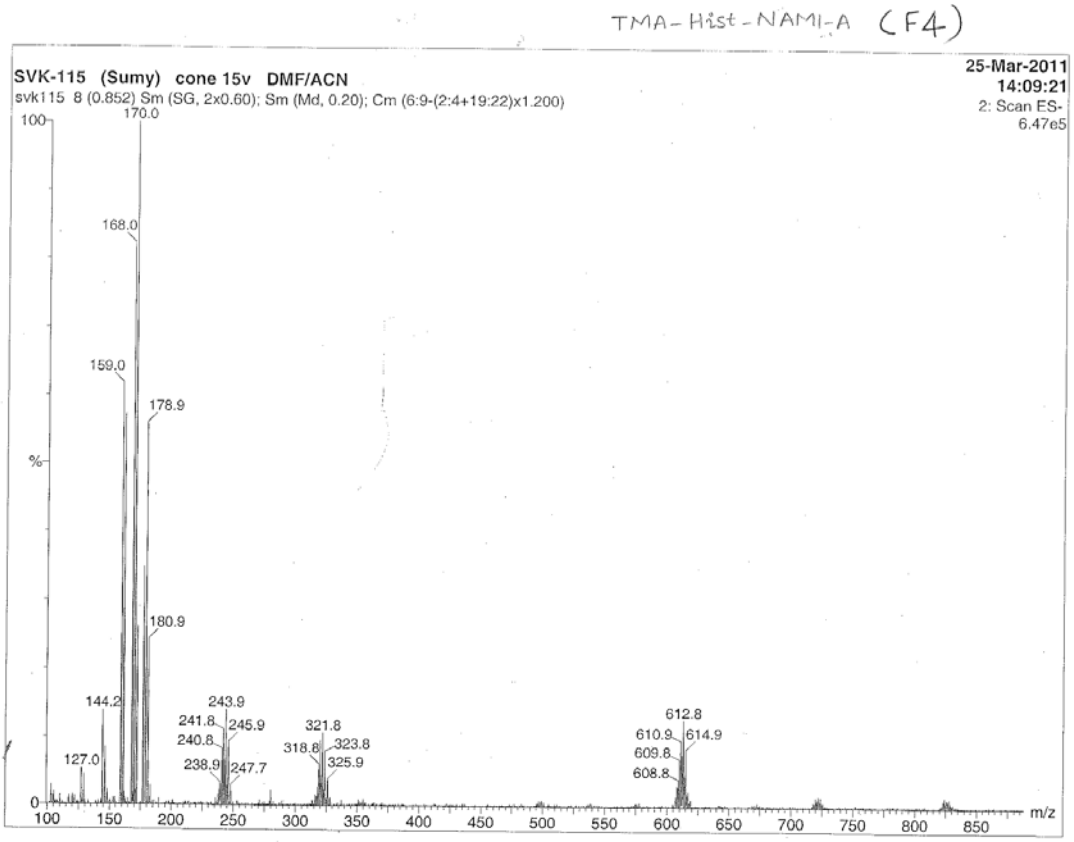

Figure S8: Electrospray mass spectrum (-ve ion) for **F4**; Cone 15V; Solvent – DMF/ACN.

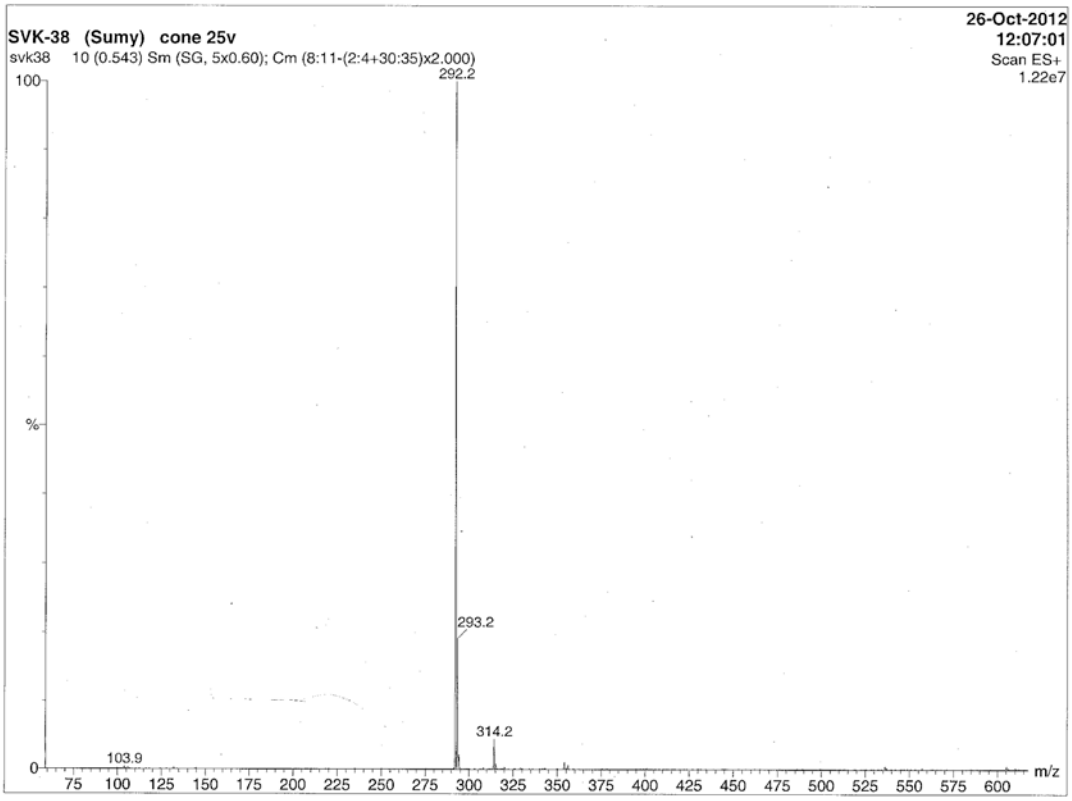

Figure S9: Electrospray mass spectrum for **F6 (N-[histaminedihydro]-1,8-naphthalenecarboximide)**; Cone 15V; Solvent – ACN.

Table SI. Summary of ESI-MS (*m/z* -ve ion) data* with fragmentation pattern

Complex	Fragment	m/z (calcd)	m/z (found)
F1	$[RuCl_4(DMSO)(7\text{-azaindole})]^-$	439.8	439.8
	$[RuCl_4(7\text{-azaindole})]^-$	361.8	361.8
	$[RuCl_4(DMSO)]^-$	321.7	321.8
	$[RuCl_4]^-$	243.7	243.8
F2	$[RuCl_4(DMSO)(\mathbf{F6})]^-$	612.8	612.8
	$[RuCl_4(DMSO)]^-$	321.7	321.8
	$[RuCl_4]^-$	243.7	243.8

*Measured by Micromass Platform II Quadruple Mass Spectrometer at cone voltage 15 V.

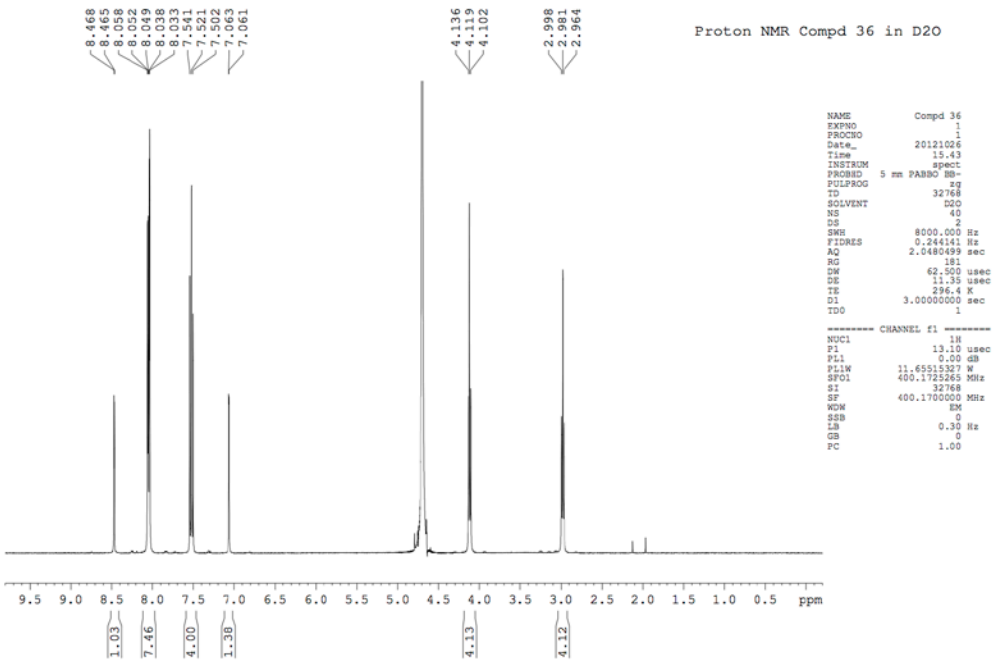

Figure S10: Proton NMR spectrum for **F6** (**N-[histaminedihydro]-1,8-naphthalenecarboximide)** in D_2O.

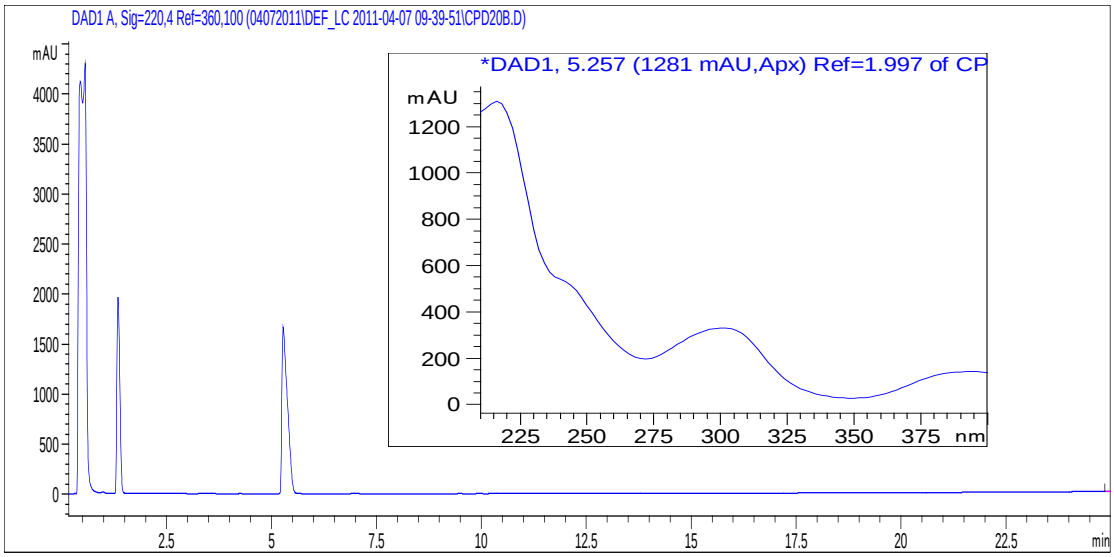

Figure S11: HPLC chromatogram of **F1** (**7-azaindolium *trans*-tetrachlorido(7-azaindole)(dimethylsulfoxide)ruthen(III)ate)** in DMF. Column: Supelco Discovery C5; Flow: 1.5 ml/min; Detection at 220 nm; Mobile phase: Buffer A (0.1% tfa/water), Buffer B (0.1%tfa/CH3CN); Gradient: 5% to 75% B, 25 minutes linear. Retention time = 1.45 and 5.15 min.

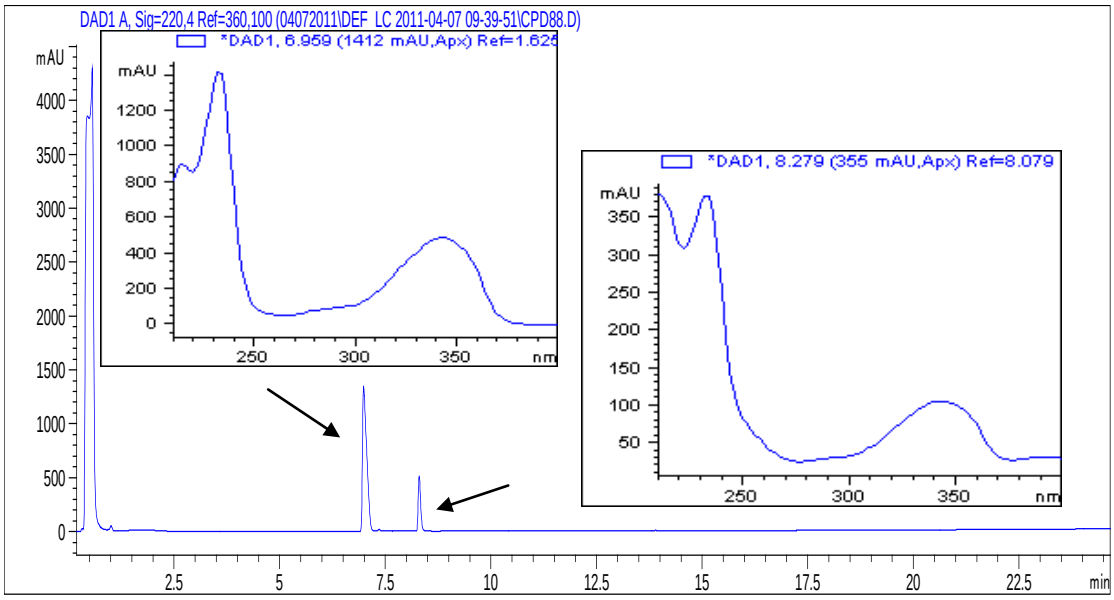

Figure S12: HPLC chromatogram of **F2** (**N-[histaminedihydrolium]-1,8-naphthalenecarboximidic *trans*-tetrachlorido(dimethylsulfoxide)(N-[histaminedihydro]-1,8-naphthalenecarboximide) ruthen(III)ate**) in DMF. Column: Supelco Discovery C5; Flow: 1.5 ml/min; Detection at 220 nm; Mobile phase: Buffer A (0.1% tfa/water), Buffer B (0.1%tfa/CH_3CN); Gradient: 5% to 75% B, 25 minutes linear. Retention time = 7 min and 8.25 min.

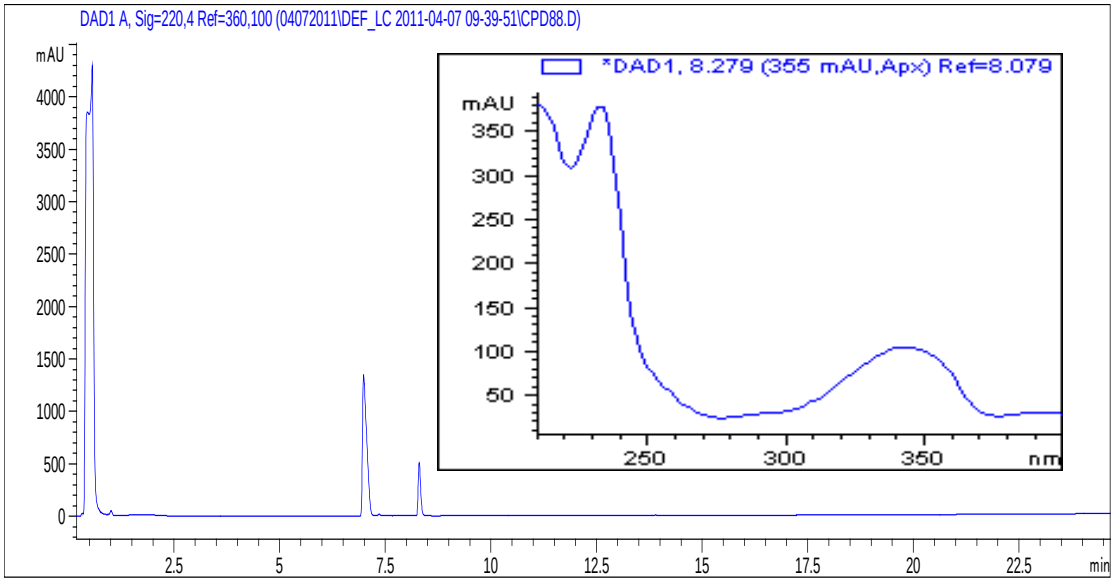

Figure S13: HPLC chromatogram of **F3 (Tetramethylammonium *trans*-tetrachlorido(7-azaindole)(dimethyl sulfoxide)ruthen(III)ate)** in DMF. Column: Supelco Discovery C5; Flow: 1.5 ml/min; Detection at 220 nm; Mobile phase: Buffer A (0.1% tfa/water), Buffer B (0.1%tfa/CH3CN); Gradient: 5% to 75% B, 25 minutes linear. Retention time = 5.3 min.

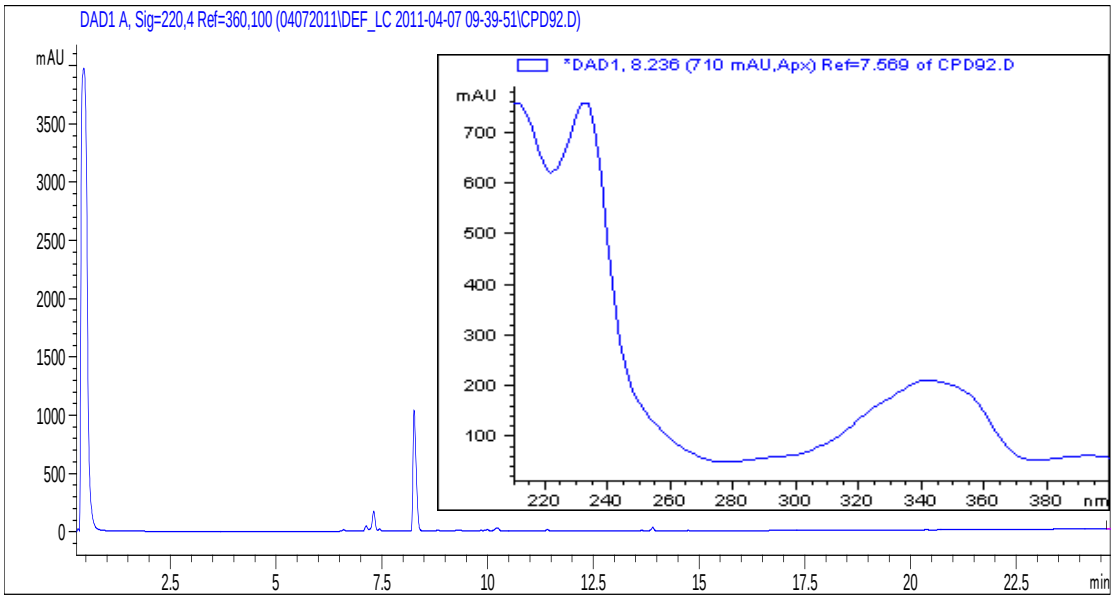

Figure S14: HPLC chromatogram of **F4 (Tetramethylammonium *trans*-tetrachlorido(dimethylsulfoxide)(N-[histaminedihydro]-1,8-naphthalenecarboximide)ruthen(III)ate)** in DMF. Column: Supelco Discovery C5; Flow: 1.5 ml/min; Detection at 220 nm; Mobile phase: Buffer A (0.1% tfa/water), Buffer B (0.1%tfa/CH3CN); Gradient: 5% to 75% B, 25 minutes linear. Retention time = 8.25 min.

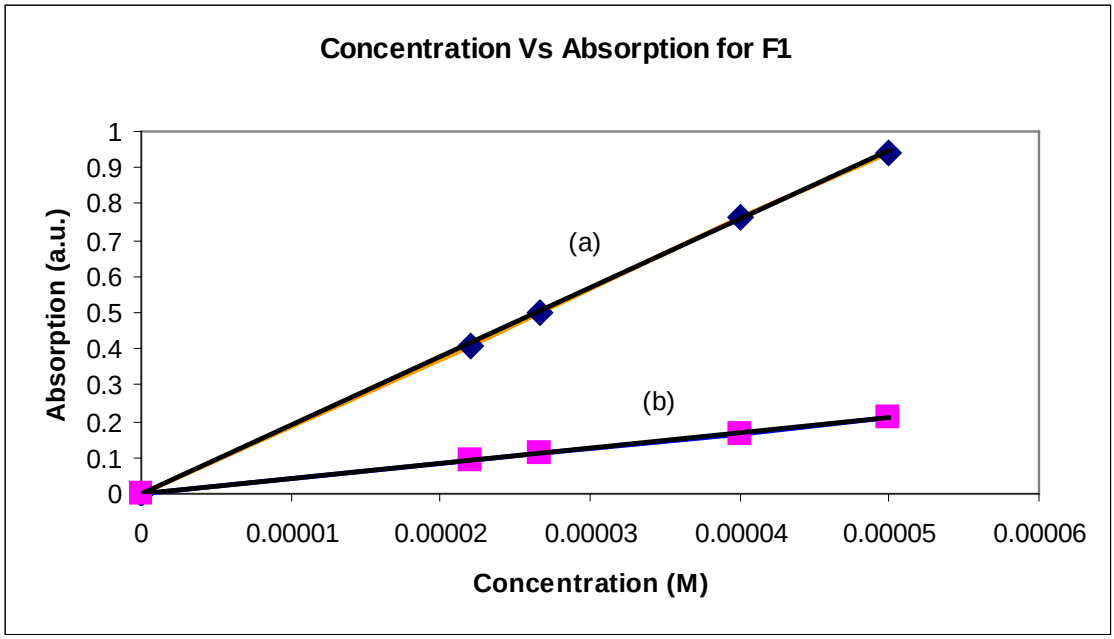

Figure S15: Effect of concentration on absorption for **F1** (7-azaindolium trans-tetrachlorido(7-azaindole)(dimethylsulfoxide)ruthen(III)ate). (a) At 291 nm; molar absorptivity (ε_{max} ; M^{-1} cm^{-1}) = 18,900 and correlation coefficient, r = 0.99. (b) At 400 nm; molar absorptivity (ε_{max} ; M^{-1} cm^{-1}) = 4,200 and correlation coefficient, r = 0.99.

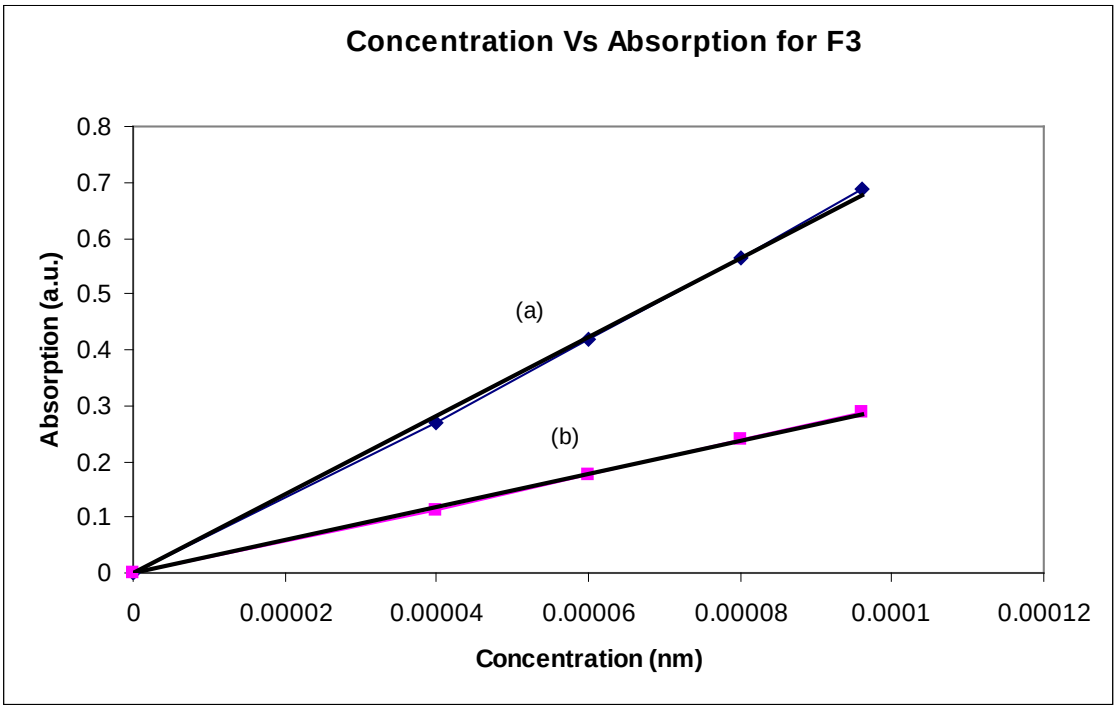

Figure S16: Effect of concentration on absorption for **F3** (Tetramethylammonium trans-tetrachlorido(7-azaindole)(dimethyl sulfoxide)ruthen(III)ate). (a) At 302 nm; molar absorptivity (ε_{max} ; M^{-1} cm^{-1}) = 7,100 and correlation coefficient, r = 0.99. (b)

At 402 nm; molar absorptivity (ε_{max} ; M^{-1} cm^{-1}) = 3,000 and correlation coefficient, r = 0.99.

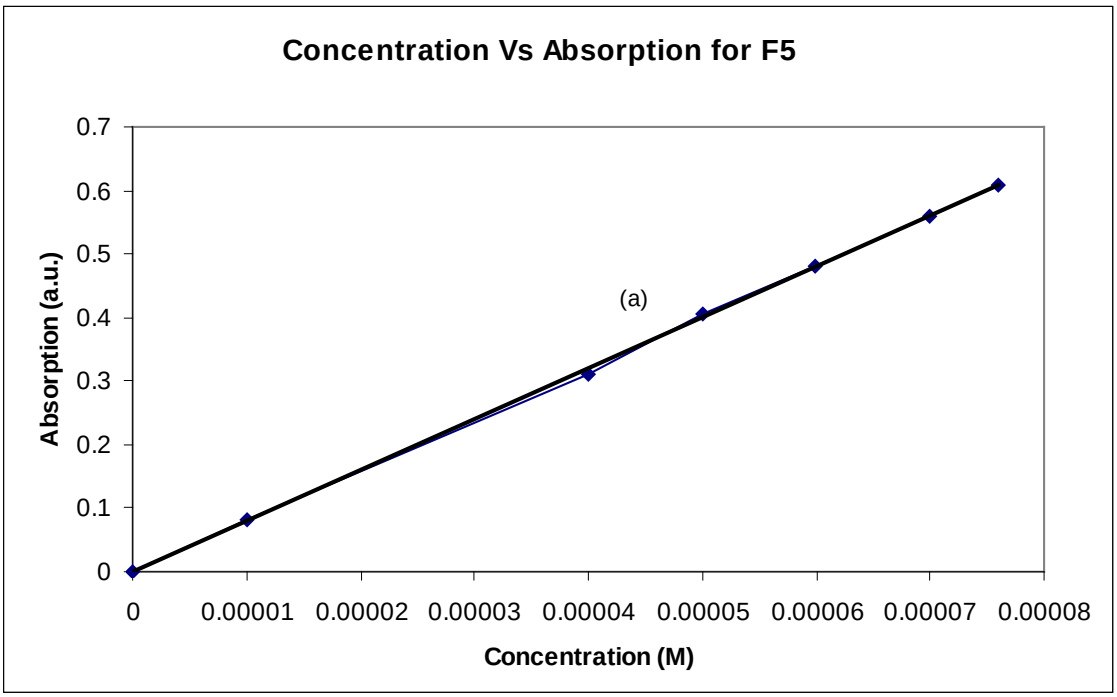

Figure S17: Effect of concentration on absorption for **F5 (7-Azaindole)**. (a) At 290 nm; molar absorptivity (ε_{max} ; M^{-1} cm^{-1}) = 8,000 and correlation coefficient, r = 0.99.

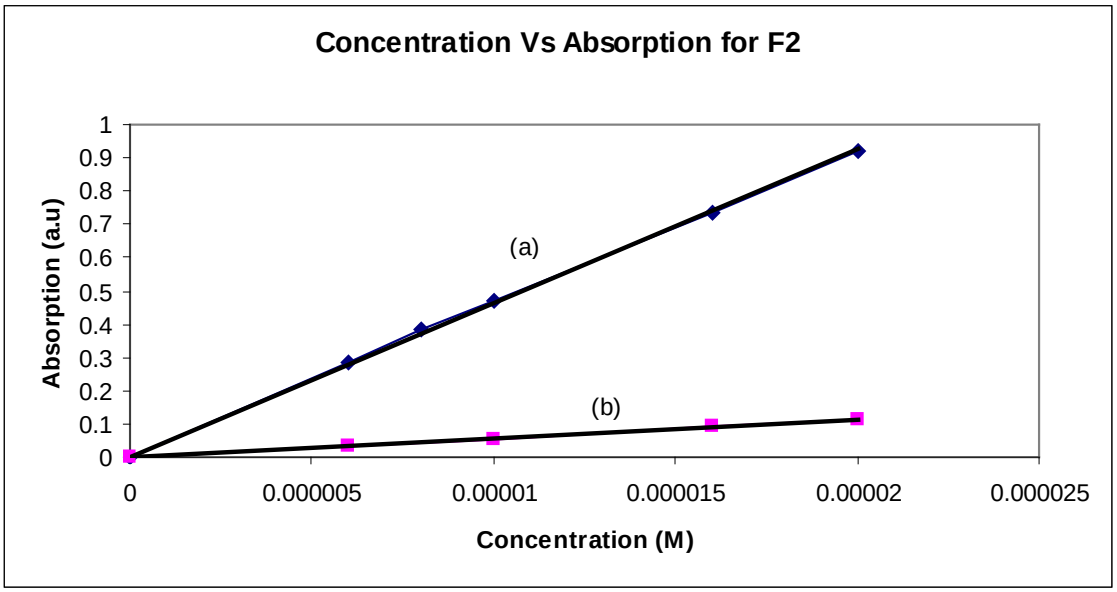

Figure S18: Effect of concentration on absorption for **F2** (N-[histaminedihydrolium]-1,8-naphthalenecarboximidic trans-tetrachlorido(dimethylsulfoxide)(N-[histaminedihydro]-1,8-naphthalenecarboximide) ruthen(III)ate). (a) At 333 nm; molar absorptivity (ε_{max} ; M^{-1} cm^{-1}) = 46,300 and correlation coefficient, r = 0.99. (b)

At 390 nm; molar absorptivity (ε_{max} ; M^{-1} cm^{-1}) = 5,600 and correlation coefficient, r = 0.99.

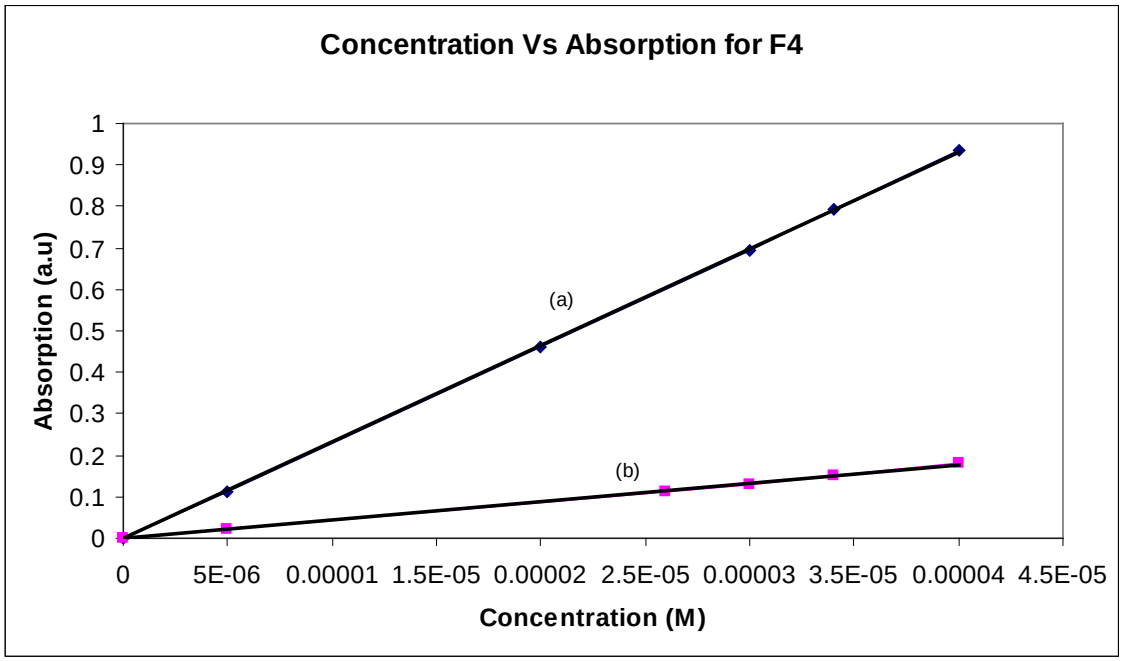

Figure S19: Effect of concentration on absorption for **F4** (Tetramethylammonium trans-tetrachlorido(dimethylsulfoxide)(N-[histaminedihydro]-1,8-naphthalenecarboximide)ruthen(III)ate). (a) At 334 nm; molar absorptivity (ε_{max} ; M^{-1} cm^{-1}) = 23,300 and correlation coefficient, r = 0.99. (b) At 375 nm; molar absorptivity (ε_{max} ; M^{-1} cm^{-1}) = 4,500 and correlation coefficient, r = 0.99.

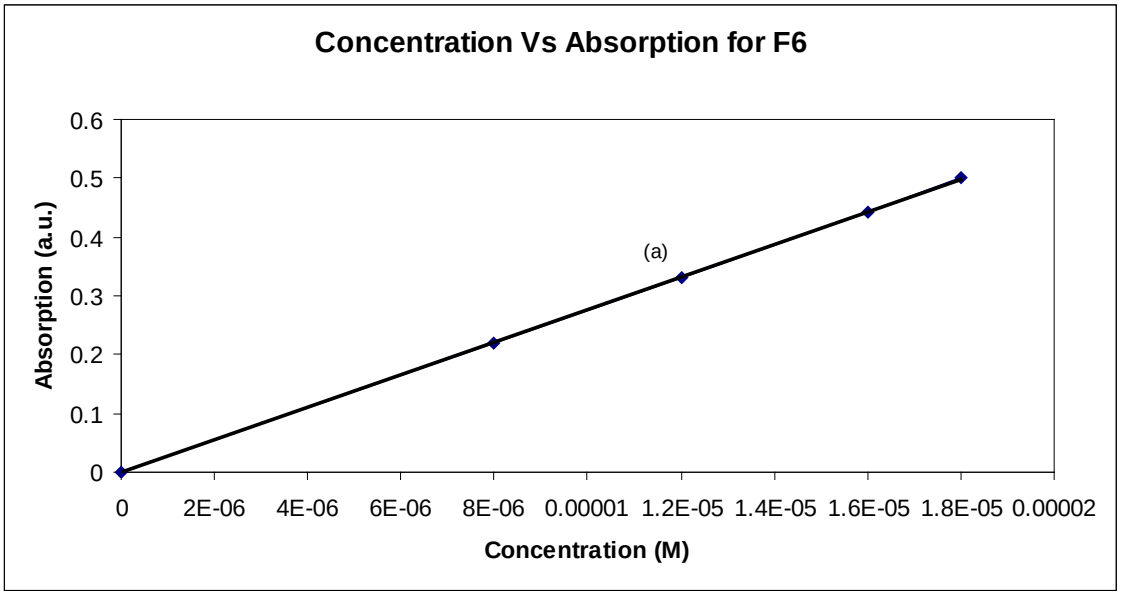

Figure S20: Effect of concentration on absorption for **F6** (N-[histaminedihydro]-1,8-naphthalenecarboximide). (a) At 332 nm; molar absorptivity (ε_{max} ; M^{-1} cm^{-1}) = 27,800 and correlation coefficient, r = 0.99.

X-ray crystal structure analysis

Crystals were grown from DMF/Methanol mixture by solvent layering method. Crystallisation of the 7-azaindole derivative (**F1; 7-azaindolium *trans*-tetrachlorido(7-azaindole)(dimethylsulfoxide)ruthen(III)ate)** caused the substitution of one chlorine molecule with one molecule of DMF. Intensity data for violet crystals of **1** (0.20 x 0.20 x 0.13 mm) were collected at 123 K on a Bruker Apex II CCD fitted with graphite monochromated Mo Kα radiation (0.71073 Å). Crystal parameters and details of the data collection are summarised in Table S2.

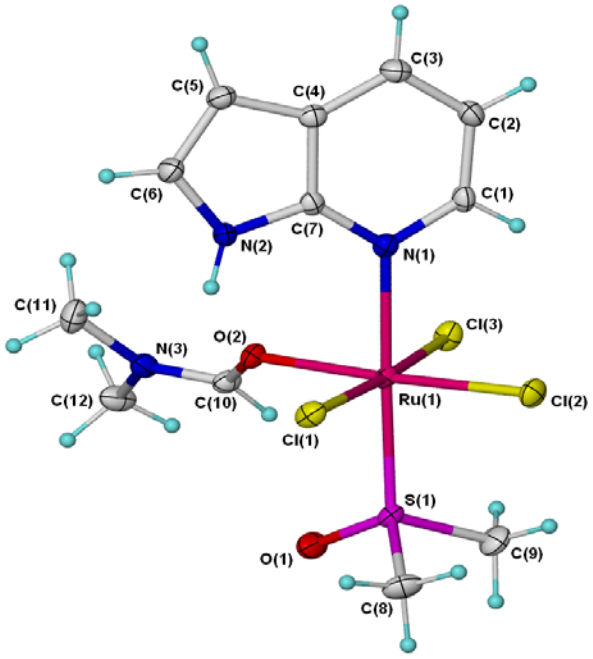

Figure S21: Molecular diagram of [$RuCl_3$(DMSO)(DMF)(7-azaindole)] with non-hydrogen atoms shown as 50% thermal ellipsoids and hydrogen atoms as spheres of arbitrary size.

Table S2: Crystal data and structure refinement for [$RuCl_3$(DMSO)(DMF)(7-azaindole)].

Crystal	**[$RuCl_3$(DMSO)(DMF)(7-azaindole)]**
Empirical formula	C12 H19 Cl3 N3 O2 Ru S
Formula weight	476.78
Temperature	123(2) K

Wavelength	0.71073 Å
Crystal system	Monoclinic
Space group	P21/*n*
Unit cell dimensions	a = 10.9531(6) Å alpha = 90^0
	b = 14.7312(4) Å beta = $93.742(7)^0$
	c = 11.0807(7) Å gamma = 90^0
Volume	1784.08(16) A^3
Z	4
Calculated density	1.775 Mg/m^3
Absorption coefficient (M(Mo Kα)/mm^{-1})	1.453 mm^{-1}
F(000)	956
Crystal size	0.20 x 0.20 x 0.13 mm
Theta range for data collection	2.30 to 32.34^0
Limiting indices	-16<=h<=15, -21<=k<=20, -8<=l<=16
Independent reflections	13501 / 5801 [*R*(int) = 0.0234]
Completeness to theta = 27.50	100.0 %
Absorption correction	Semi-empirical from equivalents
Max. and min. transmission	1.00000 and 0.88914
Refinement method	Full-matrix least-squares on F^2
Data / restraints / parameters	5801 / 1 / 207
Goodness-of-fit on F^2	1.040
Final R indices [I >2 sigma(I)]	$^aR_1$= 0.0295, $^bwR_2$ = 0.0623
R indices (all data)	$^aR_1$ = 0.0391, $^bwR_2$ = 0.0667
Largest diff. peak and hole	1.960 and -0.953 e. $Å^{-3}$

$^aR = \Sigma(|Fo| - |Fc|)/\Sigma|Fo|$. $^bR = [\Sigma w(|Fo| - |Fc|)^2/\Sigma Fo^2]^{1/2}$, where $w = [\sigma^2(Fo)]^{-1}$

Table S3. Atomic coordinates (x 10^4) and equivalent isotropic displacement parameters (A^2 x 10^3) for [$RuCl_3$(DMSO)(DMF)(7-azaindole)]. U(eq) is defined as one third of the trace of the orthogonalised Uij tensor.

	x	y	z	U(eq)
Ru(1)	2933(1)	1952(1)	5412(1)	14(1)
Cl(1)	926(1)	2059(1)	6000(1)	21(1)
Cl(2)	2444(1)	762(1)	4110(1)	22(1)

Cl(3)	4987(1)	1935(1)	4965(1)	21(1)
S(1)	2488(1)	2936(1)	3860(1)	17(1)
O(1)	2732(2)	3902(1)	4122(1)	26(1)
O(2)	3374(1)	2975(1)	6671(1)	18(1)
N(1)	3403(2)	1008(1)	6839(2)	17(1)
N(2)	2488(2)	1791(1)	8474(2)	19(1)
N(3)	4305(2)	4275(1)	7281(2)	20(1)
C(1)	4053(2)	258(1)	6608(2)	19(1)
C(2)	4390(2)	-397(2)	7458(2)	23(1)
C(3)	4060(2)	-315(2)	8638(2)	23(1)
C(4)	3409(2)	458(1)	8926(2)	19(1)
C(5)	2928(2)	812(2)	9995(2)	22(1)
C(6)	2383(2)	1614(2)	9682(2)	22(1)
C(7)	3108(2)	1094(1)	7992(2)	17(1)
C(8)	951(2)	2846(2)	3252(2)	29(1)
C(9)	3266(2)	2659(2)	2555(2)	28(1)
C(10)	4015(2)	3656(1)	6465(2)	19(1)
C(11)	3910(2)	4233(2)	8511(2)	29(1)
C(12)	5043(2)	5061(2)	6978(2)	28(1)

Table S4. Bond lengths [A] and angles [deg] for [$RuCl_3$(DMSO)(DMF)(7-azaindole)].

Ru(1)-O(2)	2.0883(14)
Ru(1)-N(1)	2.1431(17)
Ru(1)-S(1)	2.2772(5)
Ru(1)-Cl(2)	2.3115(5)
Ru(1)-Cl(3)	2.3354(5)
Ru(1)-Cl(1)	2.3387(5)
S(1)-O(1)	1.4726(16)
S(1)-C(9)	1.773(2)
S(1)-C(8)	1.777(2)
O(2)-C(10)	1.255(2)
N(1)-C(7)	1.344(2)
N(1)-C(1)	1.348(3)
N(2)-C(7)	1.360(2)
N(2)-C(6)	1.376(3)
N(3)-C(10)	1.309(3)
N(3)-C(11)	1.457(3)
N(3)-C(12)	1.463(3)
C(1)-C(2)	1.381(3)
C(2)-C(3)	1.385(3)
C(3)-C(4)	1.391(3)
C(4)-C(7)	1.418(3)
C(4)-C(5)	1.426(3)
C(5)-C(6)	1.358(3)
O(2)-Ru(1)-N(1)	86.64(6)
O(2)-Ru(1)-S(1)	94.27(4)
N(1)-Ru(1)-S(1)	177.99(5)
O(2)-Ru(1)-Cl(2)	176.69(4)
N(1)-Ru(1)-Cl(2)	90.15(5)
S(1)-Ru(1)-Cl(2)	88.955(19)
O(2)-Ru(1)-Cl(3)	88.03(4)
N(1)-Ru(1)-Cl(3)	87.77(5)
S(1)-Ru(1)-Cl(3)	90.474(19)
Cl(2)-Ru(1)-Cl(3)	92.667(19)
O(2)-Ru(1)-Cl(1)	86.92(4)

N(1)-Ru(1)-Cl(1)	91.33(5)
S(1)-Ru(1)-Cl(1)	90.505(19)
Cl(2)-Ru(1)-Cl(1)	92.339(19)
Cl(3)-Ru(1)-Cl(1)	174.915(19)
O(1)-S(1)-C(9)	106.95(11)
O(1)-S(1)-C(8)	107.60(11)
C(9)-S(1)-C(8)	99.64(12)
O(1)-S(1)-Ru(1)	116.03(7)
C(9)-S(1)-Ru(1)	112.26(8)
C(8)-S(1)-Ru(1)	112.94(8)
C(10)-O(2)-Ru(1)	124.26(13)
C(7)-N(1)-C(1)	114.82(17)
C(7)-N(1)-Ru(1)	125.39(13)
C(1)-N(1)-Ru(1)	119.79(14)
C(7)-N(2)-C(6)	108.29(17)
C(10)-N(3)-C(11)	122.90(19)
C(10)-N(3)-C(12)	120.33(19)
C(11)-N(3)-C(12)	116.76(18)
N(1)-C(1)-C(2)	124.33(19)
C(1)-C(2)-C(3)	120.6(2)
C(2)-C(3)-C(4)	117.2(2)
C(3)-C(4)-C(7)	118.12(19)
C(3)-C(4)-C(5)	135.4(2)
C(7)-C(4)-C(5)	106.45(18)
C(6)-C(5)-C(4)	106.66(18)
C(5)-C(6)-N(2)	110.49(19)
N(1)-C(7)-N(2)	126.94(18)
N(1)-C(7)-C(4)	124.94(18)
N(2)-C(7)-C(4)	108.11(18)
O(2)-C(10)-N(3)	123.0(2)

Symmetry transformations used to generate equivalent atoms:

Table S5. Anisotropic displacement parameters (A^2 x 10^3) for [$RuCl_3$(DMSO)(DMF)(7-azaindole)].

The anisotropic displacement factor exponent takes the form:
-2 pi^2 [h^2 a*^2 U11 + ... + 2 h k a* b* U12]

	U11	U22	U33	U23	U13	U12
Ru(1)	13(1)	17(1)	12(1)	-1(1)	0(1)	-3(1)
Cl(1)	15(1)	30(1)	18(1)	1(1)	2(1)	-1(1)
Cl(2)	24(1)	22(1)	20(1)	-5(1)	-2(1)	-5(1)
Cl(3)	15(1)	28(1)	21(1)	-3(1)	3(1)	-4(1)
S(1)	18(1)	20(1)	13(1)	0(1)	0(1)	-2(1)
O(1)	35(1)	18(1)	23(1)	1(1)	-3(1)	-3(1)
O(2)	19(1)	20(1)	15(1)	-3(1)	0(1)	-3(1)
N(1)	14(1)	19(1)	17(1)	-1(1)	1(1)	-1(1)
N(2)	21(1)	19(1)	16(1)	-2(1)	1(1)	5(1)
N(3)	20(1)	18(1)	22(1)	-2(1)	-4(1)	0(1)
C(1)	18(1)	21(1)	19(1)	-5(1)	2(1)	2(1)
C(2)	23(1)	21(1)	24(1)	-3(1)	-1(1)	6(1)
C(3)	25(1)	23(1)	22(1)	4(1)	-1(1)	3(1)
C(4)	18(1)	20(1)	18(1)	1(1)	-1(1)	-1(1)
C(5)	22(1)	25(1)	18(1)	1(1)	-1(1)	2(1)
C(6)	23(1)	26(1)	17(1)	-1(1)	1(1)	5(1)
C(7)	14(1)	17(1)	18(1)	-3(1)	-1(1)	-1(1)
C(8)	23(1)	39(1)	24(1)	6(1)	-8(1)	-2(1)
C(9)	34(1)	35(1)	16(1)	1(1)	7(1)	1(1)
C(10)	20(1)	20(1)	17(1)	1(1)	-4(1)	-2(1)
C(11)	29(1)	33(1)	24(1)	-9(1)	2(1)	-1(1)
C(12)	30(1)	19(1)	33(1)	3(1)	-11(1)	-5(1)

Table S6. Hydrogen coordinates (x 10^4) and isotropic displacement parameters (A^2 x 10^3) for [$RuCl_3$(DMSO)(DMF)(7-azaindole)].

	x	y	z	U(eq)
H(1)	4295	173	5808	23
H(2)	4852	-908	7231	28
H(3)	4270	-767	9227	28
H(5)	2980	541	10774	26

H(6)	1984	1998	10221	26
H(8A)	394	3013	3872	43
H(8B)	787	2219	2990	43
H(8C)	825	3255	2558	43
H(9A)	3007	3073	1896	42
H(9B)	3072	2033	2312	42
H(9C)	4150	2718	2737	42
H(10)	4303	3726	5680	23
H(11A)	3273	3769	8556	43
H(11B)	3582	4825	8733	43
H(11C)	4609	4077	9069	43
H(12A)	5321	4986	6161	42
H(12B)	5754	5108	7559	42
H(12C)	4549	5613	7012	42
H(2N)	2160(20)	2221(15)	8040(20)	28(7)